Available online at www.sciencedirect.com
SCIENCE DIRECT®
BioSystems 78 (2004) 23–37
BioSystems
www.elsevier.com/locate/biosystems

Analysis of two-component signal transduction by mathematical modeling using the *KdpD/KdpE* system of *Escherichia coli*

A. Kremling[a,*], R. Heermann[b], F. Centler[c], K. Jung[b], E.D. Gilles[a]

[a] *Systems Biology Group, Max-Planck-Institut für Dynamik Komplexer Technischer Systeme, Sandtorstr. 1; 39106 Magdeburg, Germany*
[b] *Department Biologie I, Ludwig-Maximilians-Universität München, Bereich Mikrobiologie, 80638 München, Germany*
[c] *Bio Systems Analysis Group, Department of Mathematics and Computer Science, Jena Center for Bioinformatics (JCB), Friedrich-Schiller-University Jena, 07743 Jena, Germany*

Received 12 February 2004; received in revised form 16 June 2004; accepted 25 June 2004

Abstract

A mathematical model for the *KdpD/KdpE* two-component system is presented and its dynamical behavior is analyzed. *KdpD* and *KdpE* regulate expression of the *kdpFABC* operon encoding the high affinity K^+ uptake system *KdpFABC* of *Escherichia coli*. The model is validated in a two step procedure: (i) the elements of the signal transduction part are reconstructed in vitro. Experiments with the purified sensor kinase and response regulator in presence or absence of DNA fragments comprising the response regulator binding-site are performed. (ii) The mRNA and molecule number of *KdpFABC* are determined in vivo at various extracellular K^+ concentrations. Based on the identified parameters for the in vitro system it is shown, that different time hierarchies appear which are used for model reduction. Then the model is transformed in such a way that a singular perturbation problem is formulated. The analysis of the in vivo system shows that the model can be separated into two parts (submodels which are called functional units) that are connected only in a unidirectional way. Hereby one submodel represents signal transduction while the second submodel describes the gene expression.

Keywords: *Escherichia coli*; Two-component signal transduction; Model reduction; Singular perturbation; In vivo dynamics

1. Introduction

Mathematical modeling and dynamical simulation become more and more important for the understanding of the complex behavior of metabolic and regulatory networks of cellular systems. Although there is a large qualitative knowledge, especially for bacteria, quantitative research is still scarce. Therefore, relative simple biological (sub-)systems must be analyzed to get more insight in the dynamics of intracellular processes. A number of such processes are related to the survival in a broad range of environmental conditions. Several parameters like the supply of different

* Corresponding author. Tel.: +49 391 6110 466; fax: +49 391 6110 526.
E-mail address: kremling@mpi-magdeburg.mpg.de (A. Kremling).

0303-2647/$ – see front matter © 2004 Elsevier Ireland Ltd. All rights reserved.
doi:10.1016/j.biosystems.2004.06.003

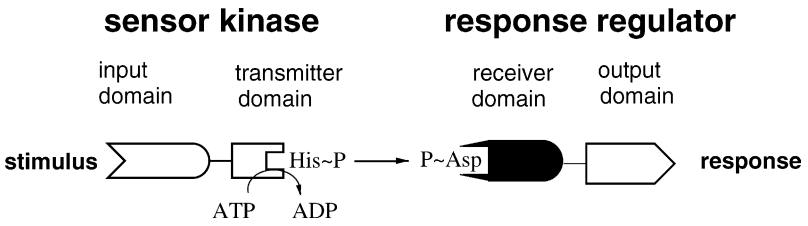

Fig. 1. General scheme of a two-component signal transduction system.

nutrients, the sudden presence of toxic substances, pH, temperature, O_2 concentration, osmolality, or different other factors can rapidly change. To survive, bacteria are forced to monitor their environment constantly and to adapt to changing conditions immediately. Therefore, bacteria have established special signal transduction systems to execute adaptive responses to changing environmental conditions. The simplest circuits consist of two protein components (two-component systems): a sensor kinase, often anchored in the cytoplasmic membrane, and a cytoplasmic response regulator that mediates an adaptive response, usually a change in gene expression (Fig. 1). Two-component systems are widespread in bacteria, archaea and plants. In *Escherichia coli*, 30 sensor kinases and 32 response regulators have been found. However, the number of two-component systems differs enormously in different bacteria, ranging from 0 in *Mycoplasma genitalium* to 80 in *Synechocystis sp.*, in which the corresponding genes account for nearly 2.5% of the genome (see Stock et al., 2000 for review). Table 1 shows a broad range of conditions and adaptive responses controlled by two-component systems in different bacteria.

Sensor kinases typically contain an N-terminal input domain which is connected via a linker to a C-terminal transmitter domain. Response regulators typically consist of a N-terminal receiver domain coupled to one ore more C-terminal output domains (Fig. 1). Upon perception of a stimulus, the input domain of the sensor kinase modulates the signaling activity of its transmitter domain, resulting in autophosphorylation of a highly conserved histidine residue with the γ-phosphoryl group of ATP. Then, the phosphoryl group is transferred to an aspartate residue of the response regulator receiver domain, resulting

Table 1
Sensor kinase/response regulator systems control various processes

Function/stress	Organism	System
Oxygen sensing	*E. coli*	ArcB/ArcA
Nitrate and nitrite respiration	*E. coli*	NarX/NarL, NarQ/NarP
Chemotaxis	Various	CheA/CheY
Nitrogen utilization	*E. coli*	NtrB/NtrC
K^+ supply	Various	*KdpD/KdpE*
Phosphate supply	Various	PhoR/PhoB; PhoQ/PhoP
Antibiotics	*Enterococcus faecium*	VanS/VanR
Osmolarity	*E. coli*, *Salmonella typhimurium*	EnvZ/OmpR
Gene transfer	*Bacillus subtilis*	ComP/ComA
Sporulation	*Bacillus subtilis*	KinB/Spo0F, KinA/Spo0F
Cell cycle	*Caulobacter crescentus*	CckA/CtrA
Photosynthetic apparatus	*Rhodobacter capsulatus*	RegB/RegA
Virulence	*Bordetella pertussis*	BvgS/BvgA
Quorum sensing	*Vibrio harveyi*	LuxN/LuxO; LuxQ/LuxO
Symbiosis	*Bradyrhizobium japonicum*	NodV/NodW
Development	*Myxococcus xanthus*	SasS/SasR

in an activation of the output domain(s) to trigger response. In most cases the response is an alteration in the transcription level of a special gene or gene cluster (see Bourret et al., 1991; Parkinson, 1993; Parkinson and Kofoid, 1992; Stock et al., 1990, 2000 for reviews).

This contribution deals with the mathematical description of a reaction mechanism representing a two-component system for the control of K^+ uptake in *E. coli*. The *KdpD/KdpE* system is one example of a typical two-component system, which regulates the expression of the *kdpFABC* operon encoding the high affinity K^+ transport system *KdpFABC* in *E. coli* most notably under K^+ limiting conditions (Walderhaug et al., 1992; Altendorf and Epstein, 1996; Jung and Altendorf, 2002). A model for two-component signal transduction was set up by (Fisher et al., 1996) earlier. They determined a number of reaction parameters for phosphotransfer from the sensor kinase VanS to the response regulators VanR and PhoB in *Enterococcus*. Models for other signal transduction systems in *E. coli* are described e.g. by Wong et al., 1997; Kremling et al., 2001; Van Dien and Keasling, 1998; Koh et al., 1998.

The strategy to set up and to analyze the mathematical model was as follows: First, the *KdpD/KdpE* signal transduction cascade was reconstructed in vitro (for details, see Appendix A). A first model was set up describing autophosphorylation of *KdpD*, transfer of the phosphoryl group between sensor kinase and response regulator, dephosphorylation of *KdpE* ∼ P, and binding of the response regulator to DNA fragments comprising the specific response regulator-binding site mentioned above. The model was validated by a set of experiments. In the second step, the overall in vivo system was analyzed. Since the *kdpFABCDE* regulon comprises the genes for the transporter as well as the sensor kinase/response regulator elements, an autocatalytic behavior was observed. The model was extended to describe mRNA and protein synthesis. The amount of mRNA and the number of transporter molecules inside the cell were determined experimentally. The mathematical model was used to analyze time scales of the stimulus response. To evaluate the quality of the model, steady-state values of the concentration of the K^+ uptake system for different stress conditions were calculated and compared with experimental data.

2. Model equations for the in vitro system

Although it is known that during enzymatic activities proteins form a number of temporary complexes, in this contribution a rather simple reaction mechanism was used to describe the two-component system (Fig. 2). Incorporating such temporary complexes increases the number of unknown parameters. Since for cellular systems measurements of the system components are difficult and only a subset of components can be measured, the model structure should also be as simple as possible to facilitate parameter identification (Saez-Rodriguez et al., 2004).

The reaction equations are:

Autophosphorylation :

$$\mathrm{ATP} + KdpD \underset{k_{-1}}{\overset{k_1}{\rightleftarrows}} \mathrm{ADP} + KdpD^p \qquad \text{(R1)}$$

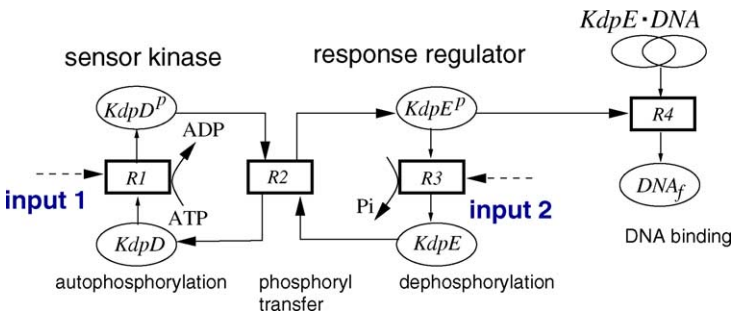

Fig. 2. The reaction mechanism for the *KdpD/KdpE* two-component system. The ellipses represent proteins. Two putative input loci are under consideration. Input 1 describes alterations of the kinase activity while input 2 describes the alterations of the phosphatase activity. The phosphorylated response regulator binds upstream of the *kdpFABC* promoter/operator region and in interaction with the RNA polymerase triggers *kdpFABC* expression. The reactions denoted as autophosphorylation, phosphoryl transfer, dephosphorylation and DNA binding are described in the text.

Phosphoryl group transfer :

$$KdpD^p + KdpE \underset{k_{-2}}{\overset{k_2}{\rightleftarrows}} KdpD + KdpE^p \quad \text{(R2)}$$

Dephosphorylation:

$$KdpE^p + KdpD \xrightarrow{k_3} KdpE + KdpD\,(+\mathrm{P}_i) \quad \text{(R3)}$$

DNA binding:

$$2\,KdpE^p + \mathrm{DNA}_f \underset{k_{-b}}{\overset{k_b}{\rightleftarrows}} KdpE - \mathrm{DNA} \quad \text{(R4)}$$

For the *KdpD/KdpE* system it is yet not known at which stage the stimulus enters the system and two possible input loci are under consideration (denoted in the following as input 1 and input 2). In this contribution only one stress condition is under investigation and therefore the stimulus is represented as a fixed parameter. In reaction R1 the stimulus (via input 1) enhances the kinase activity that results in autophosphorylation of the sensor kinase (state variables *KdpD*, $KdpD^p$) by ATP. In reaction R2 the phosphoryl group is transferred to the response-regulator (state variables *KdpE*, $KdpE^p$). $KdpE \sim \mathrm{P}$ contains the active output domain. It is known that *KdpE* can be phosphorylated by alternative phosphor donors in the presence of an truncated form of *KdpD* (Heermann et al., 2003). However, this phosphorylation plays a minor role in the presence or absence of *KdpD*. Because of this uncertainty, phosphorylation of *KdpE* by acetyl phosphate and other low molecular weight phosphordonors was not included into the model. The dephosphorylation of $KdpE \sim \mathrm{P}$ by the cognate sensor kinase *KdpD* is described in reaction R3 (controlled via input 2: decrease of dephosphorylation). It has been shown earlier that $KdpE \sim \mathrm{P}$ dephosphorylation is only dependent on *KdpD* (Jung et al., 1997), so that other phosphatases are not considered in the model. Note that, although the stoichiometry of the back reaction of R2 and reaction R3 are similar, the underlying mechanisms are different: for R3 it is assumed that *KdpD* acts as an enzyme converting a substrate ($KdpE \sim \mathrm{P}$) into products (*KdpE* and P_i) while in R2 the phosphoryl group is transferred between the regulatory proteins. Hence, the reaction rate for R3 (parameter k_3) is not included in the balance equation for the sensor. However, high values of the phosphorylated sensor $KdpD \sim \mathrm{P}$ results in low values for the free form of the sensor and therefore leads to a decreased rate of dephosphorylation. An intrinsic rate of dephosphorylation, i.e. a decay of the phosphorylated response regulator was not observed (Puppe et al., 1996). The activated response regulator forms a dimer and is then able to bind to the free DNA (state variable DNA_f) in reaction R4 to build a transcription complex (state variable $KdpE - \mathrm{DNA}$). Non-specific binding of the response regulator to other DNA binding sites could be neglected in the model (experimental data not shown).

The equations for the system are assorted in the following. For the total concentration of the kinase $KdpD_0$ and of the response regulator $KdpD_0$ the following equations hold:

$$KdpD_0 = KdpD + KdpD^p \quad (1)$$

$$KdpE_0 = KdpE + KdpE^p + 2KdpE - \mathrm{DNA} \quad (2)$$

And for the entire concentration of the DNA fragments DNA_0:

$$\mathrm{DNA}_0 = \mathrm{DNA}_f + KdpE - \mathrm{DNA} \quad (3)$$

The three remaining differential equations read:

$$\frac{\mathrm{d}KdpD^p}{\mathrm{d}t} = -k_{-1}KdpD^p\,\mathrm{ADP} - k_2\,KdpD^p\,KdpD + k_1\,KdpD\,\mathrm{ATP} + k_{-2}\,KdpD\,KdpE^p \quad (4)$$

$$\frac{\mathrm{d}KdpE^p}{\mathrm{d}t} = -k_{-2}\,KdpD\,KdpE^p - k_3\,KdpE^p\,KdpD - 2\,k_b\,KdpE^{p2}\,\mathrm{DNA}_f + k_2\,KdpD^p\,KdpE + 2\,k_{-b}\,KdpE - \mathrm{DNA} \quad (5)$$

$$\frac{\mathrm{d}KdpE - \mathrm{DNA}}{\mathrm{d}t} = -k_{-b}\,KdpE - \mathrm{DNA} + k_b KdpE^{p2}\,\mathrm{DNA}_f \quad (6)$$

To compare situations in vivo and in vitro and to study the influence of the phosphoryl source, ATP is taken as a constant parameter value although it is consumed in minor amounts during the in vitro reaction.

2.1. Parameter estimation and results

The goal of parameter estimation is to find a set of parameters that can describe the experimental results. Here, it was based on the following experiments. The complete signal transduction cascade was reconstructed in vitro (see Appendix A for experimental details). Briefly, purified and reconstituted *KdpD*

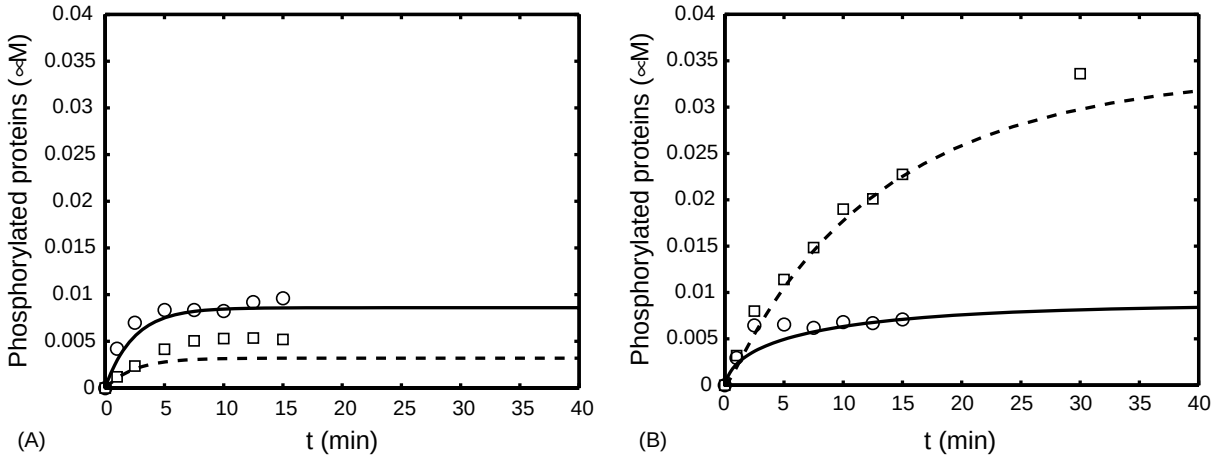

Fig. 3. Experimental and simulation results for the in vitro system. (A) Stress situation (0 mM K^+), no DNA fragments comprising the chromosomal *KdpE*-binding site were present. (B) Stress situation (0 mM K^+), in the presence of DNA fragments. Solid lines: simulation of phosphorylated *KdpD*, dashed lines: simulation of phosphorylated *KdpE*, circles: experimental data for phosphorylated *KdpD*, squares: experimental data for phosphorylated *KdpE*.

was mixed with purified *KdpE* (ratio 1:4). Then, an ATP/ADP mixture (ratio 12.5:1) was added, and the amounts of phosphorylated sensor kinase and response regulator were determined over time (Fig. 3). Two experiments were performed: one in the absence and one in the presence of DNA fragments comprising the response regulator-binding site. In both experiments phosphorylated *KdpD* was detectable albeit at very low amounts. In the presence of DNA fragments comprising the *KdpE*-binding site, the amount of phosphorylated *KdpE* was about 10 times higher as in the absence of these DNA fragments after 30 min.

Subsequently, we searched for one set of parameters that described these experimental results. Parameter values fitted with a least-square algorithm (MATLAB©) are summarized in Table 2. To have an impression on the quality of the fitted parameters, a sensitivity analysis was performed according to the method Hearne (Hearne, 1985). The method seeks a perturbed parameter vector to maximize the disturbance to the solution trajectory. Therefore, the method is useful for analyzing effects of a combination of parameter changes on the system. The parameters with the highest sensitivity were k_1, k_3, k_b and k_{-b}.

2.2. Model analysis and model reduction

2.2.1. Stationary behavior

In the described experiment a low degree of phosphorylation (<1%) was observed. However, the conditions used in the in vitro experiments did not reflect situations expected in vivo. Therefore, to reproduce intracellular conditions the influence of the ATP concentration on the steady-state values of the phosphorylated response regulator was under investigation. Fig. 4 shows steady-state values of the degree of phosphorylation $KdpE^p/KdpE_0$ in dependence on the ATP concentration. As can be seen, under in vivo conditions (>1.5 mM) a considerable higher degree of phosphorylation is expected. Such high ATP concentrations could not be adjusted in vitro, because by further addition of cold ATP, no measurement signal can be detected.

2.2.2. Singular perturbation problem

For the understanding of the overall behavior of cellular systems, mathematical models can be used to de-

Table 2
Parameter values for the in vitro data set

In vitro parameters	
k_1 = 0.0029 1/h μM	DNA_0 = 100 μM
k_{-1} = 0.00088 1/h μM	$KdpD_0$ = 1 μM
k_2 = 108 1/h μM	$KdpE_0$ = 4 μM
k_{-2} = 1080 1/h μM	ATP = 100 μM
k_b = 5400 1/h μM^2	ADP = 8 μM
k_{-b} = 360 1/h	
k_3 = 90 1/h μM	(0 mM K^+/no DNA)
k_3 = 90 1/h μM	(0 mM K^+/DNA)

Parameters were estimated with a least square algorithm.

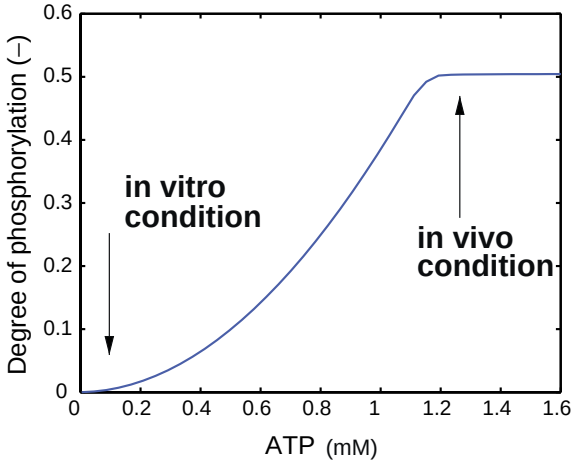

Fig. 4. Steady-state behavior of the system. The degree of phosphorylation is defined as $KdpE^p/KdpE_0$. For in vivo conditions the degree of phosphorylation is much higher than for the conditions used in vitro.

tect new ("emergent") properties. A first step in model analysis is model reduction, i.e. to come to a "simpler" description of the system. Here, the number of independent states (the order of the system) is reduced by coupling two (or more) states by algebraic equations. One possibility to obtain algebraic equations is to analyze the time hierarchies of the system and to regard fast modes—in comparison to the chosen time window—as in steady-state.

To illustrate the approach, the scheme is simplified. Only two reactions are considered. Reaction (A1) describes phosphorylation and dephosphorylation of a response regulator rp from a general source s (constant entity) and reaction (A2) describes the interaction of rp with the DNA binding-site:

$$\text{synthesis:} \qquad s \underset{k_-}{\overset{k}{\rightleftarrows}} rp \tag{A1}$$

$$\text{DNA–binding:} \qquad rp \underset{k_{-b}}{\overset{k_b}{\rightleftarrows}} rd \tag{A2}$$

Scaling the O.D.E.s with $dt = 1/k\, d\tau$, and rearranging leads to the system:

$$rp' = s - K\, rp - \frac{k_b}{k}\,(rp - K_b\, rd) \tag{7}$$

$$rd' = \frac{k_b}{k}\,(rp - K_b\, rd)\,, \tag{8}$$

with $K = k_-/k$ and $K_b = k_{-b}/k_b$. Introducing a new state $r = rp + rd$ leads to a singular perturbation problem with $\epsilon = k/k_b$:

$$r' = s - K\,(r - rd) \tag{9}$$

$$\epsilon\, rd' = r - (1 + K_b) rd. \tag{10}$$

For very small ϵ it is allowed to perform a model reduction with $\epsilon = 0$. The system (A1,A2) can be rewritten with one O.D.E. for r:

$$r' = s - K(r - rd) \tag{11}$$

and one algebraic equation for rd:

$$rd = \frac{r}{1 + K_b}. \tag{12}$$

For the overall original model (R1)–(R4), scaling was performed with $dt = 1/k_2\, KdpE_0\, d\tau$ and based on the fitted set of parameter $\epsilon = k_2/k_b\, KdpE_0 \approx 5 \times 10^{-3}$. Model reduction for the original system is then equivalent to the assumption that reaction (R4) is in rapid equilibrium:

$$KdpE^{p2}\,\mathrm{DNA}_f = K_b\, KdpE - \mathrm{DNA}. \tag{13}$$

Thereby, the system is reduced to two O.D.E.s for $KdpD^p$ and $KdpE^p$, two algebraic equations to calculate the free amount of DNA (DNA_f), and unbound response regulators ($KdpEs_f^p$) and two algebraic equations for the total amount of sensor kinase and response regulator:

$$\frac{d\, KdpD^p}{dt} = -k_{-1}\, KdpD^p\,\mathrm{ADP} - k_2\, KdpD^p\, KdpE + k_1\, KdpD\,\mathrm{ATP} + k_{-2}\, KdpD\, KdpE_f^p \tag{14}$$

$$\frac{d\, KdpE^p}{dt} = -k_{-2}\, KdpD\, KdpE_f^p - k_3\, KdpE_f^p\, KdpD + k_2\, KdpD^p\, KdpE \tag{15}$$

$$KdpE^p = KdpE_f^p + 2\frac{KdpE_f^{p2}\,\mathrm{DNA}_f}{K_b} \tag{16}$$

$$\mathrm{DNA}_0 = \mathrm{DNA}_f + \frac{KdpE_f^{p2}\,\mathrm{DNA}_f}{K_b}, \tag{17}$$

where $K_b = k_{-b}/k_b$ is the binding affinity of $KdpE_f^p$ to the binding site DNA_f. The two algebraic equations for the total amount of sensor kinase and response regulator read:

$$KdpD_0 = KdpD + KdpD^p \tag{18}$$

$$KdpE_0 = KdpE + KdpE^p. \tag{19}$$

Differences during simulation experiments between the two models could hardly be detected (data not shown).

3. Model equations for the in vivo system

To describe the overall system in vivo, the model was extended with equations for the mRNA (state variable RNA)

$$\text{RNA: (nucleotides)} \xrightarrow{r_{tr}} \text{RNA} \xrightarrow{k_z} \text{degradation} \tag{20}$$

and the dynamical equations for the proteins *KdpFABC* ($KdpF$), total *KdpD* ($KdpD_0$), and total *KdpE* ($KdpE_0$)

$$KdpFABC\text{: (amino acids)} \xrightarrow{r_{tl1}} KdpF \xrightarrow{k_d} \text{degradation} \tag{21}$$

$$KdpD\text{: (amino acids)} \xrightarrow{r_{tl2}} KdpD_0 \xrightarrow{k_d} \text{degradation} \tag{22}$$

$$KdpE\text{: (amino acids)} \xrightarrow{r_{tl3}} KdpE_0 \xrightarrow{k_d} \text{degradation} \tag{23}$$

The organisation of the *kdpFABCDE* regulon is shown in Fig. 5. Under *kdpFABC*-inducing conditions a transcript *kdpFABC* is formed, and probably by a read-through effect the transcription of *kdpDE* is also enhanced. Indeed, under K^+-limiting growth conditions, increased amounts of *KdpD* and *KdpE* are detectable (unpublished information). This is taken into account in equations (22) and (23). The existence of a putative terminator was analyzed but could not be detected (data not shown). However, different molecule numbers of the transport system, sensor kinase and response regulator are expected although they are co-regulated. This is considered by different values for the translation efficiency.

Since it is assumed that the concentration of nucleotides and amino acids are not limiting, the rate laws r_{tr} and r_{tl_i} do not depend on the monomer concentration. To describe transcription efficiency based on the interaction of a number of response regulators a new method that was introduced previously was used to calculate the rate of mRNA synthesis r_{tr} (see Section 3.1). To describe translation efficiency the following approach is used:

$$r_{tl_i} = k_{tl_i}\,\mathrm{RNA}, \tag{24}$$

while for protein degradation a first order law with parameter k_d is used.

3.1. Brief summary of the modeling approach to describe transcription initiation

The method is based on the hierarchical structure of the regulatory network and calculates the transcription efficiency by neglecting unimportant interactions between regulator proteins and DNA-binding

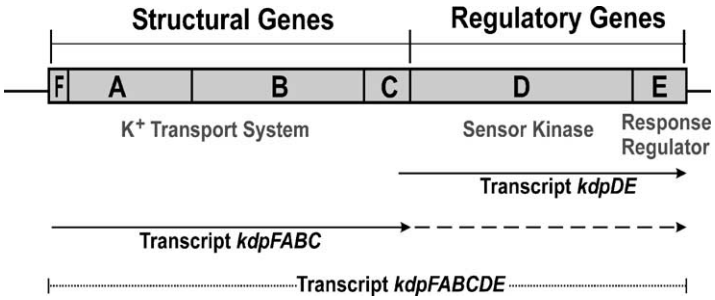

Fig. 5. Schematic representation of the *kdpFABCDE* regulon. The *kdpDE* operon is transcribed from its own promoter. Under *kdpFABC*-inducing conditions a transcript *kdpFABC* is formed, and the transcription of *kdpDE* is enhanced, probably by a read-through effect.

sites (Kremling and Gilles, 2001). Since the RNA polymerase is essential for transcription, it represents the cellular or top level while other regulator proteins have a special function (or are more specific) in metabolism, they are e.g. activators or inhibitors for the expression of specific genes. These regulator proteins are therefore assigned to further levels in the hierarchy. The hierarchical model structure allows a signal transduction from the top to the lowest level but not vice versa. Therefore, some interactions of the proteins are neglected which leads to a simpler model structure in comparison to a complete model, including all interactions.

The model used here assumes that the amount of RNA polymerase and the concentration of the σ factor are constant entities. Therefore, a basic activity of the RNA polymerase is considered by state ψ (the value is fixed). The interaction of the regulator with the DNA-binding sites enhances RNA polymerase activity (state $\bar{\psi}$). The equations to derive an expression for $\bar{\psi}$ are given in the Appendix A. The following equation will hold for the rate of mRNA synthesis r_{tr}:

$$r_{tr} = k_{tr}\,\bar{\psi}\,\mathrm{DNA}_0. \tag{25}$$

The rate of transcription is proportional to the RNA polymerase activity and the number of templates.

The O.D.E.s for the in vivo system read:

$$\frac{d\mathrm{RNA}}{\mathrm{d}t} = k_{tr}\,\bar{\psi}\,\mathrm{DNA}_0 - (k_z + \mu)\,\mathrm{RNA} \tag{26}$$

$$\frac{\mathrm{d}KdpD_0}{\mathrm{d}t} = k_{tl2}\mathrm{RNA} - (k_d + \mu)S_0 \tag{27}$$

$$\frac{\mathrm{d}KdpE_0}{\mathrm{d}t} = k_{tl3}\,\mathrm{RNA} - (k_d + \mu)R_0 \tag{28}$$

$$\frac{\mathrm{dKdpF}}{\mathrm{d}t} = k_{tl1}\,\mathrm{RNA} - (k_d + \mu)F, \tag{29}$$

where μ is the specific growth rate during the experiment.

The concentration of the mRNA was determined by Northern blot analysis. Therefore, an additional equation for mRNA^m (state variable RNA^m) was used to relate the measured quantity to the mRNA concentration.

$$\mathrm{RNA}^m = k_m\,\mathrm{RNA} \tag{30}$$

Parameter k_m was estimated based on data on mRNA synthesis from *E. coli* (Bremer and Dennis, 1987).

The dynamical equations for $KdpD^p$ and $KdpE^p$ read:

$$\frac{\mathrm{d}KdpD^p}{\mathrm{d}t} = -k_{-1}\,KdpD^p\,\mathrm{ADP} - k_2\,KdpD^p\,KdpE + k_1\,KdpD\,\mathrm{ATP} + k_{-2}\,KdpD\,KdpE^p \tag{31}$$

$$\frac{\mathrm{d}KdpE^p}{\mathrm{d}t} = -k_{-2}\,KdpD\,KdpE^p - k_3\,KdpE^p\,KdpD + k_2\,KdpD^p\,KdpE \tag{32}$$

Note that Eqs. (14) and (15) are similar to Eqs. (31) and (32) except for using $KdpE^p$ instead $KdpE_f^p$ on the right side. Explanation in Section 4.

3.2. Parameter estimation and results

The measured time course for the mRNA concentration shows an interesting unexpected dynamic (Fig. 6). After reaching a maximum at 10 min mRNA decreases until a new steady-state is reached after approximatly 40 min. Since the current structure of the model is not able to describe the observation, a hypothesis was formulated to describe the measured data: the decrease of the mRNA concentration could only be explained when a reset is assumed. Since the model does not include the participation of a functional transporter in any way it is assumed here, that the transport of K^+ ions mediated by *KdpFABC* counteracts the stimulus. Since no information on possible detailed mechanisms is available, an empirical black-box approach is used. Fig. 7 shows an extended scheme used to describe the mRNA dynamics.

For the black box the following mathematical expression is used: assuming that the stimulus enters the system by the dephosphorylation of the response regulator (parameter k_3), an increase of the intracellular K^+ concentration mediated by the K^+ uptake system *KdpFABC* should increase this parameter with increasing transporter concentration resulting in a dephosphorylation of *KdpE*. This is described by the following equation:

$$k_3 = k_h \frac{KdpF}{KdpF + K_h}, \tag{33}$$

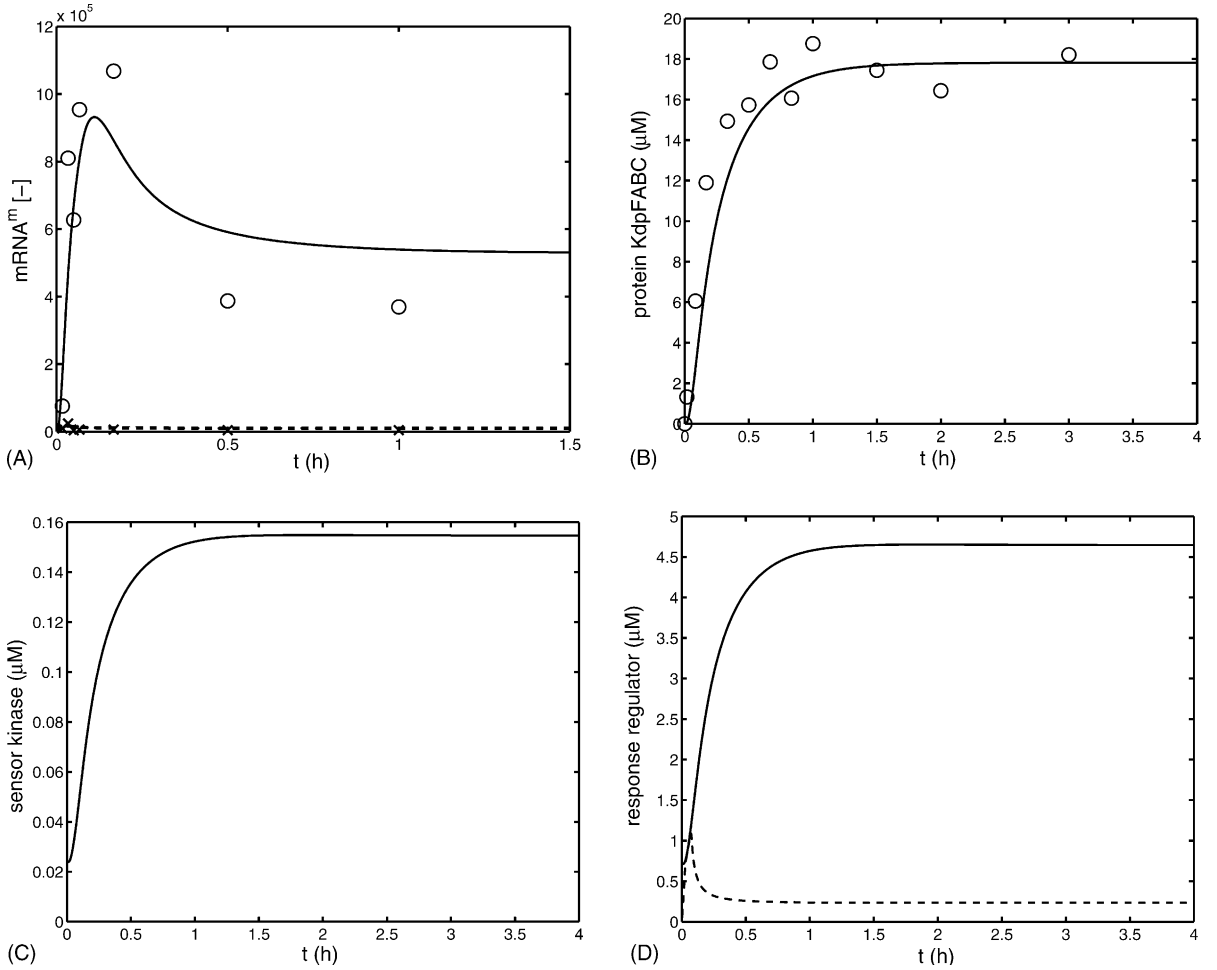

Fig. 6. Experimental and simulation results of the extended in vivo system. (A) Time course of mRNA^m. Circles represent an experiment under K^+ limiting conditions, solid line represents the simulation result; crosses represent an experiment during uninduced conditions, dashed line represents the simulation result. (B) Time course of protein *KdpFABC*. Solid lines: simulation results under K^+-limiting conditions, circles: experimental data under K^+-limiting conditions. (C) Time course of simulated sensor kinase. (D) Time course of simulated response regulator. Solid line represents the entire concentration of the response regulator, dashed line represents the phosphorylated response regulator.

where k_h and K_h represent adjustable parameters. The second putative input via the phosphorylation of the sensor kinase is not considered further. Parameter k_1 is taken as a constant.

Based on the available in vivo experimental data, parameters for the expression velocity could be determined by least-square parameter fit (MATLAB©). However, simulation studies with the in vitro parameters lead to unrealistic results. Therefore, parameters of autophosphorylation and phosphoryl transfer were estimated, while the parameters for DNA binding were fixed to the values estimated for the in vitro system. For the in vivo system measurements for the sensor kinase and response regulator were not available and estimation of all parameters of the two-component unit seems not feasible. Parameters k_{-1} and k_{-2} are therfore taken out of the list of parameters that were estimated while they are fixed to empirical values. Since data are only available for the amount of protein *KdpFABC* the following assumption is made:

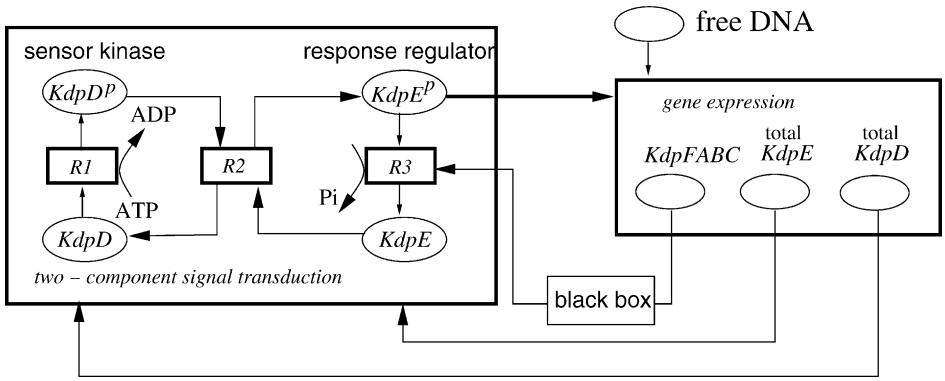

Fig. 7. The extended reaction mechanism for the two-component system. The model describes the expression of the proteins *KdpFABC*, *KdpD* and *KdpE*. The total amount of sensor kinase and response regulator are now further inputs in the two-component module. Due to unexpected dynamics of the mRNA a black box model is introduced describing a possible feedback from the transporter to the two-component module.

the number of molecules of *KdpE* have a fixed ratio $ra = 0.26$ to the number of molecules of *KdpFABC*, i.e. the concentration of the response regulator is assumed to be *ra* times the concentration of *KdpFABC*. The ratio between sensor kinase and response regulator is 1/30 ((Polarek et al., 1992) & unpublished own results).

In Fig. 6 simulation and experimental results are shown for a K^+ concentration $c_{K^+} = 0.02$ mM in the medium (parameters in Table 3, the values for ATP and ADP are chosen to be 2 mM and 0.2 mM, respectively). The time course of the mRNA and protein *KdpFABC* is reproduced with the model very well. To calculate the basal activity of the promoter, represented by pa-

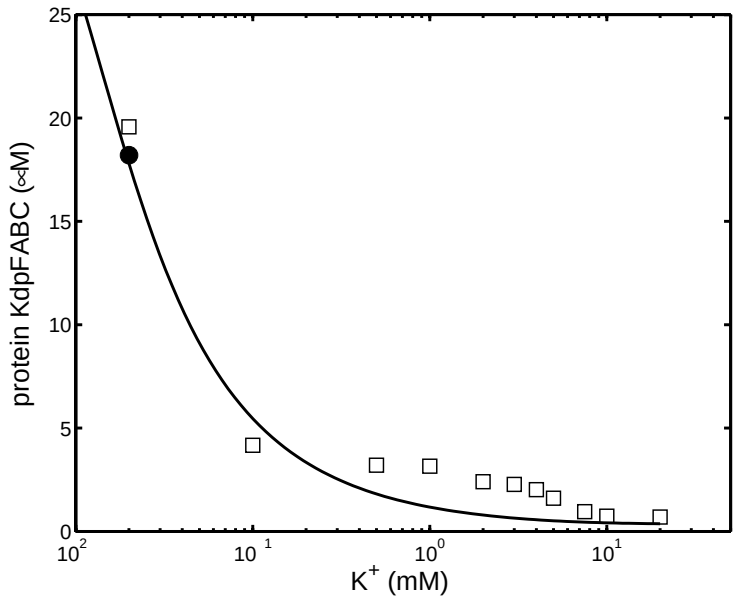

Fig. 8. Experimental data and simulation prediction for *KdpFABC* under different stress situations. Plotted are steady-state values against K^+ concentration. Squares: experimental data of steady-state values, closed circle: final value for *KdpFABC* taken from Fig. 6, solid line represents simulation results.

Table 3
Parameters for the in vivo data set

In vivo parameters	
k_1 = 248.39 1/h μM	DNA_0 = 0.0054 μM[b]
$k_{-1} = 10^{-4}$ 1/h μM[a]	ψ = 0.0017
k_2 = 5789.3 1/h μM	α = 0.008
k_{-2} = 0.041 1/h μM[a]	ATP = 2 mM[b]
K_b = 0.0667 μM^{2}[d]	ADP = 0.2 mM[b]
k_{tr} = 2000 1/h[e]	k_z = 28.87 1/h
k_{tl1} = 1150 1/h	k_d = 1.51 1/h
k_{tl2} = 10 1/h	k_{tl3} = 300 1/h
k_h = 9982.5 1/h μM	K_h = 0.04 μM[a]
$k_m = 6.97 \cdot 10^9$	μ = 0.5 1/h[c]

Parameters were estimated with a least-square algorithm ([a]empirical values, [b]intracellular concentrations, [c]experimental, [d]taken from the in vitro experiment, [e]taken from (Bremer and Dennis, 1987)).

rameter ψ in the model, the mRNA was measured also during uninduced conditions (see also Fig. 6 left hand side). The value obtained, $\psi = 0.0017$, is comparable to a value obtained for the lac operon (Kremling et al., 2001).

To evaluate the quality of the model, the steady-state concentration of the uptake system *KdpFABC* was determined experimentally and compared to simulation predictions under different stress conditions. In the model the value for k_h is increased proportional to the increase of the stimulus concentration c_{K^+} according to the formula:

$$k_h = k_h^0 \frac{c_{K^+}}{c_{K^+}^0} \tag{34}$$

where k_h^0, $c_{K^+}^0$ represent the conditions given for the experiment in Fig. 6.

Fig. 8 compares the experimental and simulation results. A remarkable similarity of both curves was observed. Increasing the K^+ concentration in the medium to 1 mM results in a shut off of gene transcription while for higher K^+ concentrations a minor change of the steady-state values was observed.

4. Discussion

In this contribution a complete signal transduction pathway in *E. coli* starting from the sensory element to the cellular response is under investigation. For several reasons the Kdp system was chosen as an ideal test system:

- the signal transduction pathway is very short, it comprises only two elements;
- the signal transduction pathway could be reconstructed in vitro and is therefore accessible for measurements under two conditions (in the presence and absence of DNA fragments);
- the cellular response, i.e. the number of molecules of *KdpFABC* could be measured in vivo as well as the amount of *kdpFABC* mRNA under different stress conditions.

A mathematical model was set up to describe the experimental results. The model has a rather simple structure: temporary complexes between ATP and sensor kinase or between sensor kinase and response regulator were neglected to reduce the number of unknown or uncertain parameters. Parameters were estimated based on a number of experiments. For most experiments a good agreement between simulation and measurement data was achieved. For concentrations of K^+ between $0.5\,\text{mM} < c_{K^+}^0 < 5\,\text{mM}$ the residuals are larger. This is based on the fact, that these measurements were not used in the fitting procedure described above.

The in vitro experiments have shown a very low degree of phosphorylation. This might be due to two reasons: the ATP concentration used in the experiments didn't match intracellular conditions. In Fig. 4 the degree of phosphorylation is extrapolated to represent intracellular conditions. A degree of phosphorylation of nearly 50% could be achieved. On the other hand, as can be seen in Fig. 3 the amount of DNA shifts the equilibrium to the phosphorylated component. However, in an intracellular environment the number of binding sites for the response regulator is rather low and therefore could not result in a higher degree of phosphorylation.

Model reduction is always a powerful tool to reduce the degree of freedom in dynamical systems. Here, we applied the singular perturbation approach to show that different time hierarchies appear in the system under investigation. The analysis led to a system with O.D.E.s coupled with (implicit) algebraic equations, i.e. the dynamics of the binding of the response regulator is a "mirror" of the dynamics of the autophosphorylation and phosphoryl transfer.

In Kremling et al. (2000) we proposed a general framework to decompose metabolic and regulatory net-

works into functional units. Functional units are representing submodels with limited autonomy. One of the aspects under investigation considers signal transduction and describes the process of transcription initiation in Kremling et al. (2000) described with a modeling object called "coordinator" with an input/output relation. The aim of the decomposition is the definition of a set of submodels with fixed attributes which are the basis for a computer tool that support the modeler in setting up complex models (Kremling et al., 2001). Based on the analysis of the proposed mathematical model for the two-component system a reduced model comprising algebraic equations and O.D.E.s was developed. The reduced model consists out of two submodels which are connected in both directions in the in vitro case: submodel 1 describes the signal transduction to activate the response regulator while submodel 2 describes the interaction of the activated response regulator with the DNA control sequence. Analyzing the system in vivo shows however, that both units can be linked in a one-way direction. This is based on the fact that the in vivo amount of the DNA-binding site is very small in comparison to the DNA amount used in vitro. This leads to the observation that the concentration of $KdpE^p$ and of $KdpE_f^p$ in the reduced model are nearly equal, i.e. only a minor number of molecules is bound to the DNA. A decomposition of a more complex signal transduction pathway for catabolite repression was shown in (Kremling et al., 2000). However, in this paper the decomposition was based on biologically motivated criteria. Here, we show that there is also a theoretical basis that will allow the separation in different submodels.

Since the sensor kinase and the response regulator are auto-controlled, the dynamics of mRNA synthesis strongly depends on the initial conditions. Values used are in the expected range described in the literature (≈ 0 molecules sensor kinase, 300 molecules response regulator (Polarek et al., 1992) & unpublished own results). The low number of molecules makes it necessary to use a stochastic modeling approach. This was done and the results were compared with the deterministic approach. Differences could hardly be detected (data not shown). A good agreement between the experimental results and the simulated time course of the state variables was achieved by assuming a feedback from the protein *KdpFABC* to the input. In this way the model can be used for an experimental design to evaluate this hypothesis. For this purpose a mutant strain, defective in the uptake of K^+ via the KdpFABC system will be used. When the hypothesis is correct a monotone increase of the mRNA concentration is expected.

Parameter values estimated in the in vitro case led to unrealistic results in the in vivo case. This is mainly based on the fact that in vitro the phosphorylation degree of *KdpE* was very low (0.5%). Parameters used for in vitro case therefore lead to a very slow accumulation of the mRNA in contrast to the observed experimental results shown in Fig. 6. Hence, some of the parameters had to be identified again. For the parameter fit, two experiments with low and high K^+ concentration were used. Simulation results of the response regulator at a low K^+ concentration showed that that degree of phosphorylation reaches nearly 100% at the very beginning of the experiment (Fig. 6), and reaches a steady value of approximately 5%. A high degree of phosphorylation seems to be necessary for a quick response to environmental conditions. Based on the results, a steady-state characteristic curve was predicted with the model and finally compared with experimental results (Fig. 8). Here, also a good agreement was achieved.

Two-component signal transduction is one of the important mechanisms for bacteria to sense their environment and to respond to altered conditions. The present study gives some insights into the dynamics of such systems and can be used as starting conditions for other systems.

Acknowledgements

This work was supported by the Deutsche Forschungsgemeinschaft [JU 270/4-1 (K.J.)] and the Fonds der Chemischen Industrie. We thank Mechthild Krabusch for excellent technical assistance and Britta Hasemeier for providing data for Fig. 6.

Appendix A

A.1. Additional equations for the in vivo system

The proposed method to calculate the transcription efficiency $\bar{\psi}$ is based on two algebraic equations

(16,17). They are extended in the following way:

$$KdpE^{p} = KdpE^{p}{}_{f} + 2\,\frac{KdpE^{p2}_{f}\,\mathrm{DNA}_{f}}{K_{b}}\left(1+\frac{1}{\alpha\,K}\right) \tag{A.1}$$

$$\mathrm{DNA}_{0} = \mathrm{DNA}_{f}\left(1+\frac{1}{K}\right) + \frac{KdpE^{p2}_{f}\,\mathrm{DNA}_{f}}{K_{b}}\left(1+\frac{1}{\alpha\,K}\right), \tag{A.2}$$

where parameter $K = (1-\psi)/\psi$ represents the basal activity of the RNA polymerase and parameter α is an amplification factor. Transcription can occur if RNA polymerase is active alone or together with the activator. Hence, the fraction $\bar{\psi}$ of occupied promoter is given by:

$$\bar{\psi} = \frac{\mathrm{DNA}_{f}}{K\cdot\mathrm{DNA}_{0}}\left(1+\frac{KdpE^{p2}_{f}}{\alpha\,K_{b}}\right). \tag{A.3}$$

A.2. Reconstruction of the KdpD/KdpE signal transduction cascade in vitro

We reconstructed the complete signal transduction cascade of the *KdpD/KdpE* system in vitro. Purified *KdpD* (Jung et al., 1997) in proteoliposomes and purified *KdpE* (Heermann et al., 2003) in a ratio of 1 to 4 μM were mixed with 100 μM DNA comprising the DNA-binding site of *KdpE* (Sugiura et al., 1992) in buffer (50 mM Tris/HCl pH, 7.5, 10% glycerol (v/v), 0.5 M NaCl, 2 mM dithiotreitol). The double-stranded DNA fragments comprising the *KdpE*-binding sites were obtained by annealing of two complementary oligonucleotides. The upper strand sequence (from 5′ to 3′) has the following sequence: 5′-CATTTTTATACTTTTTTTACACCCCGCCCG-3′. The reaction was started by addition of 100 μM [γ-^{32}P]ATP (0.476 Ci/mmol), 8 μM ADP (ratio of 1 to 12.5, reflecting the ratio in living cells), and 110 μM $MgCl_2$. At the times indicated, samples were taken and the reactions were stopped by addition of an equal volume of 2× concentrated sodium dodecyl sulfate (SDS) sample buffer (Laemmli, 1970). In each case, samples were immediately subjected to SDS polyacrylamide gel electrophoresis (Laemmli, 1970). Gels were dried, the amount of radio-labeled proteins was detected by exposure of the gels to a phosphor screen, and the images were analyzed with a PhosphorImager SI system (Molecular Dynamics) using [γ-^{32}P]ATP as a standard. In parallel, the phosphorylation degree of *KdpE* ∼ P was determined in a gel-free detection system. This method consists of direct spotting of the phosphorylated sample on nitrocellulose after removal of *KdpD* ∼ P (ultracentrifugation) and [γ-^{32}]P ATP (gel filtration).

A.3. Quantification of the produced KdpFABC complex

Expression of *kdpFABC* was measured at the translational level by quantitative Western blot analysis. *E. coli* K-12 cells were grown at 37 °C in phosphate-buffered minimal medium (Epstein and Kim, 1971) containing 10 mM K^+ until the mid-exponential phase, filtered and resuspended in pre-warmed medium of lower K^+ concentration (0.02 mM K^+), and harvested at the indicated time. To measure the amount of *KdpFABC* complex in steady state, cells were grown in minimal media containing the indicated K^+ concentrations, and harvested at an absorbance of ≈1.0 at 600 nm. Cells were resuspended in SDS sample buffer and subjected to SDS–polyacrylamide gel electrophoresis (Laemmli, 1970). Quantification of *KdpFABC* was basically performed following the protocol developed for lactose permease (Sun et al., 1996). Briefly, proteins were electro-blotted to a nitrocellulose membrane. Blots were then blocked with 5% (w/v) bovine serum albumin (BSA) in 10 mM Tris/HCl (pH 7.5)/0.15 M NaCl (buffer A) for 1 h. Anti-KdpB antibody was added at a final dilution of 1:5000, and incubation was continued for 1 h. After washing with buffer A, ^{125}I-protein A (Amersham Biosciences) was added at a final dilution of 1:5000, and incubation was continued for 1 h. After washing thoroughly, the membrane was exposed to a phosphor screen. Known amounts of purified *KdpFABC* complex were used to obtain a standard curve. The amount of *KdpFABC* complex was then quantified using the PhosphorImager SI system (Molecular Dynamics) by comparison to the standard curve.

A.4. Quantification of kdpFABC mRNA

For quantification of the produced *kdpFABC* mRNA under K^+-limiting conditions, *E. coli* K-12 cells were

grown at 37 °C in phosphate-buffered minimal medium (Epstein and Kim, 1971) containing 10 mM K^+ until the mid-exponential phase, filtered, and subsequently resuspended in medium of lower K^+ concentration (0.02 mM K^+) or the same medium as before (10 mM K^+). At the indicated times, cells were harvested and the RNA was prepared according to (Aiba et al., 1981). For quantitative Northern blot analysis, 20 μg of RNA from each sample was separated by electrophoresis in 1.2% (w/v) agarose-1.1 M formaldehyde gels in MOPS (morpholinepropanesulfonic acid) buffer. Equal loading of samples onto the gel was verified by ethidium bromide staining of the rRNA in a separate gel. RNA was transferred to Hybond-N nylon membrane (Amersham Biosciences) by upward capillary action. Hybridization was performed following a standard protocol (Sambrock et al., 1989) using γ-^{32}P-radio-labeled dCTP PCR fragments as specific probes for kdpA (nt 1009 to 1794). Radioactivity was quantified with the PhosphorImager SI (Molecular Dynamics).

References

Aiba, H., Adhya, S., de Crombrugghe, B., 1981. Evidence for two functional gal promoters in intact *E. coli* cells. J. Biol. Chem.

Altendorf, K., Epstein, W., 1996. The KdpATPase of *Escherichia coli*. In: Dalbey, R.E. (Eds.), Advances in Cell and Molecular Biology of Membranes and Organelles. JAI Press, vol. 5, Greenwich, London, pp. 401–418.

Bourret, R.B., Borkovich, K.A., Simon, M.I., 1991. Signal transduction pathways involving protein phosphorylation in prokaryotes. Annu. Rev. Biochem. 60, 401–441.

Bremer, H., Dennis, P.P., 1987. Modulation of chemical composition and other parameters of the cell by growth rate. In: Neidhardt, F.C. (Ed.), (Editor in Chief) *Escherichia coli* and *Salmonella typhimurium*. ASM Press, Washington, DC, pp. 1527–1542.

Van Dien, S.J., Keasling, J.D., 1998. A dynamic model of the *Escherichia coli* phosphate-starvation response. J. Theor. Biol. 190, 37–49.

Epstein, W., Kim, B.S., 1971. Potassium transport loci in *Escherichia coli* K-12. J. Bacteriol. 108, 639–644.

Fisher, S.L., Kim, S.-K.K., Wanner, B.L., Walsh, C.T., 1996. Kinetic comparison of the specifity of the vanomycin resistance kinase VanS for two response regulators. VanR and PhoB. Biochemistry 35, 4732–4740.

Hearne, J.W., 1985. Sensitivity analysis of parameter combinations. Appl. Math. Modelling 9, 106–108.

Heermann, R., Altendorf, K., Jung, K., 2003. The N-terminal input domain of the sensor kinase *KdpD* of *Escherichia coli* stabilizes the interaction between the cognate response regulator *KdpE* and the corresponding DNA-binding site. J. Biol. Chem. 278 (51), 51277–51284.

Jung, K., Altendorf, K., 2002. Towards an understanding of the molecular mechanisms of stimulus perception and signal transduction by the *KdpD/KdpE* system of *Escherichia coli*. J. Mol. Microbiol. Biotechnol. 4, 223–228.

Jung, K., Tjaden, B., Altendorf, K., 1997. Purification, reconstitution, and characterization of *KdpD*, the turgor sensor of *Escherichia coli*. J. Biol. Chem. 272, 10847–10852.

Koh, B.T., Tan, R.B.H., Yap, M.G.S., 1998. Genetically structured mathematical modeling of trp attenuator mechanism. Biotechnol. Bioeng. 58, 502–509.

Kremling, A., Bettenbrock, K., Laube, B., Jahreis, K., Lengeler, J.W., Gilles, E.D., 2001. The organization of metabolic reaction networks. Part III. Application for diauxic growth on glucose and lactose. Metab. Eng. 3 (4), 362–379.

Kremling, A., Gilles, E.D., 2001. The organization of metabolic reaction networks. Part II. Signal processing in hierarchical structured functional units. Metab. Eng. 3 (2), 138–150.

Kremling, A., Jahreis, K., Lengeler, J.W., Gilles, E.D., 2000. The organization of metabolic reaction networks: a signal-oriented approach to cellular models. Metab. Eng. 2 (3), 190–200.

Laemmli, U.K., 1970. Cleavage of structural proteins during the assembly of the head of bacteriophage T4. Nature 227, 680–685.

Parkinson, J.S., 1993. Signal transduction schemes of bacteria. Cell 73 (5), 857–871.

Parkinson, J.S., Kofoid, E.C., 1992. Communication modules in bacterial signaling proteins. Annu. Rev. Genet. 26, 71–112.

Polarek, J.W., Williams, G., Epstein, W., 1992. The products of the *kdpDE* operon are required for expression of the Kdp ATPase of *Escherichia coli*. J. Bacteriol. 174 (7), 2145–2151.

Puppe, W., Jung, K., Lucassen, M., Altendorf, K., 1996. Characterization of truncated forms of the *KdpD* protein, the sensor kinase of the K^+-translocating Kdp system of *Escherichia coli*. J. Biol. Chem. 271, 25027–25034.

Saez-Rodriguez, J., Kremling, A., Gilles, E.D., Dissecting the puzzle of life: Modularization of signal transduction networks. Comput. Chem. Eng., 2004. in press.

Sambrock, J., Fritsch, E.F., Maniatis, T., Molecular cloning: a laboratory manual. Cold Spring Harbor Laboratory, Cold Spring Harbor, NY, 1989.

Stock, A.M., Robinson, V.L., Goudreau, P.N., 2000. Two-component signal transduction. Annu. Rev. Biochem. 69, 183–215.

Stock, J.B., Stock, A.M., Mottonen, J.M., 1990. Signal transduction in bacteria. Nature 344, 395–400.

Sugiura, A., Nakashima, K., Tanaka, K., Mizuno, T., 1992. Clarification of the structural and functional features of the osmoregulated kdp operon of *Escherichia coli*. Mol. Microbiol. 6, 1769–1776.

Sun, J., Wu, J., Carrasco, N., Kaback, H.R., 1996. Identification of the epitope for monoclonal antibody 4B1 which uncouples lactose and proton translocation in the lactose permease of *Escherichia coli*. Biochemistry 35, 990–998.

Walderhaug, M.O., Polarek, J.W., Voelkner, P., Daniel, J.M., Hesse, J.E., Altendorf, K., Epstein, W., 1992. *KdpD* and *KdpE*, proteins that control expression of the *kdpABC* operon, are members of the two-component sensor-effector class regulators. J. Bacteriol. 174, 2152–2159.

Wong, P., Gladney, S., Keasling, J.D., 1997. Mathematical model of the lac operon: Inducer exclusion, catabolite repression, and diauxic growth on glucose and lactose. Biotechnol. Prog. 13, 132–143.